Experiments in Robust Unbalance Response Control

Carl R. Knospe and Samir M. Tamer

Center for Magnetic Bearings, Department of Mechanical, Aerospace, and Nuclear Engineering,
University of Virginia, Charlottesville, Virginia, 22903, U.S.A.
tel: 01-804-982-2603; fax: 01-804-982-2246; e-mail: crk4y@virginia.edu

Abstract: The stability and performance robustness of an algorithm for the suppression of unbalance induced vibration of rotors supported in magnetic bearings is examined in a series of experiments. The results are used to validate previously reported analysis and synthesis tools. The synthesis results produce an adaptation algorithm gain matrix which is robust to structured uncertainty in the rotor. Three synthesized gain matrices were tested. Each resulted in significantly greater robustness than the standard solution of the problem. The experimental results also demonstrate that the degree of stability and performance robustness obtained with the synthesized gain matrices was very close to that specified in the design procedure.

1 Introduction

1.1 Background

Many researchers have tackled the problem of controlling unbalance vibration via magnetic bearings [1-5]. For this problem, adaptive open loop control (AOLC) methods have shown a great deal of promise. Here, synchronous perturbation control signals are generated and added to the feedback control signals so as to minimize the rotor unbalance response. Recently, the authors have demonstrated that the stability and performance robustness of an AOLC algorithm can be analyzed using structured singular value methods [6] and that these methods may be extended to provide a synthesis procedure for the design of the AOLC gain matrix [7]. Herein, we review the robustness theory for these systems and present experimental results which demonstrate the effectiveness of the analysis and synthesis procedure.

1.2 Mathematical Notation

The two-norm of a vector v is indicated by the notation $\|v\|$. The maximum singular value of a matrix P is denoted by $\bar{\sigma}(P)$ and the spectral norm by $\rho(P)$. The lower and upper linear fractional transformations [8] of P are given the notations $\mathcal{F}_l(P,Q)$ and $\mathcal{F}_u(P,R)$ respectively where the matrices Q and R are assumed to be appropriately dimensioned. The Redheffer star-product of appropriately dimensioned matrices P and Q will be denoted by $\mathrm{S}(P,Q)$. The structured singular value [8] of a matrix P is indicated by the notation $\mu_\Delta(P)$. The symbol S_Δ is used to denote the set of all matrices of a defined block structure.

2 Adaptive Open Loop Control

The control algorithm uses a model of the rotor system where vibration is related to the applied open loop signals via

$$X_i = TU_i + X_{0_i} \tag{1}$$

where X, X_0, and U are respectively vectors of the (complex) synchronous Fourier coefficients of the vibration measurements, the uncontrolled vibration, and the applied unbalance response control signals (dimensions: $X \in C^n, X_0 \in C^n, U \in C^m$). The matrix T is a $n \times m$ matrix of complex influence coefficients. The subscript i will be used to denote the i'th update of the control and the corresponding synchronous response. The influence coefficient matrix is the transfer function matrix of the supported rotor (with feedback control) from perturbation forces at the bearings to the displacements at the sensors, evaluated at the rotor operating speed Ω.

The applied synchronous control signals are updated using the *adaptation* law

$$U_{i+1} = U_i + AX_i \tag{2}$$

where A is the gain matrix. This form of adaptive open loop control is called *convergent control*. The standard approach for determining the gain matrix A is through minimization of the quadratic performance function $J = X^*X$ which results in the optimal gain matrix [5]

$$A \equiv -\left[T^*T\right]^{-1} T^* \tag{3}$$

The best synchronous performance that can be obtained through active control as measured by the minimum value of the quadratic performance index is denoted J_{opt}

$$J_{opt} = X^*_{opt} X_{opt} \qquad X_{opt} = \left[I - T\left(T^*T\right)^{-1} T^* \right] X_o$$

For implementation, an estimate of the matrix T, denoted $\hat{T}$, must be used. This estimate yields the *nominal system optimal* (NSO) gain matrix

$$A_{nso} = -\left[\hat{T}^*\hat{T}\right]^{-1}\hat{T}^* \tag{4}$$

When the estimate is in error, the adaptation process, governed by Eqns. (1) and (2), results in the control vector either growing unbounded (*unstable adaptation*) or converging to a control vector U_n that may not be equal to the optimal control vector (*stable adaptation*). A necessary and sufficient condition for stability is $\rho(I + AT) < 1$. A sufficient condition for adaptation process stability is given by the following condition [6]:

$$\bar{\sigma}(I + AT) < \varepsilon_c \qquad \varepsilon_c \le 1 \tag{5}$$

where ε_c is the convergence rate. This more conservative condition is required to obtain an upper bound on worst case performance. If the adaptation process is stable, the steady state value of the vibration vector is given by

$$X_n = \left[I - T(AT)^{-1} A \right] X_{opt} \tag{6}$$

3 Robustness Analysis

A structured uncertainty representation will be used. That is, several parameters $\theta_1, \theta_2, \ldots \theta_i, \cdots \theta_p$ of the state space model are different from the nominal values $\bar{\theta}_i$ that produced the influence coefficient estimate $\hat{T}$ and this difference is bounded as follows

$$\theta_i = \bar{\theta}_i + k_i \delta_i$$
$$|\delta_i| \le 1 \qquad \delta_i \in C \text{ or } \delta_i \in R$$

where k_i are real scaling factors. If the state space model of the rotor system is affinely dependent on the parameter uncertainties $\delta_1, \delta_2, \ldots \delta_i, \cdots \delta_p$, then the influence coefficient matrix of the rotor system can be represented by a linear fractional transformation (LFT) of the following form [6]

$$T = \mathcal{F}_u\left(G(j\Omega), \Delta_s\right)$$
$$\equiv G_{22}(j\Omega) + G_{21}(j\Omega)\Delta_s\left[I - G_{11}(j\Omega)\Delta_s\right]^{-1} G_{12}(j\Omega)$$

where $G_{22}(j\Omega) = \hat{T}$ and Δ_s is a block diagonal matrix of the parameters' uncertainties. Throughout the remainder of this paper, the notation $(j\Omega)$ will be suppressed.

Theorem 1: Stability Robustness
The adaptation process has exponential convergence with convergence rate ε_c for all T given by the family of matrices

$$T = \mathcal{F}_u(G, \Delta_s) \qquad \Delta_s \in S_{\Delta_s}: \ \bar{\sigma}(\Delta_s) \le 1 \tag{7}$$

if and only if

$$\mu_\Delta(S_a) < 1$$

$$S_a \equiv S(G,V) \qquad V \equiv \begin{bmatrix} 0 & I \\ \frac{1}{\varepsilon_c}A & \frac{1}{\varepsilon_c}I \end{bmatrix} \qquad \Delta = \begin{bmatrix} \Delta_s & \\ & \Delta_f \end{bmatrix} \tag{8}$$

where Δ_s is a structured block representing the parametric uncertainty, $\Delta_s \in S_{\Delta_s}$, and Δ_f is a full complex block, $\Delta_f \in C^{m\times m}$.
Proof : See [6].

Theorem 2: Performance Robustness
If the performance is measured using a quadratic performance index of the steady state vibration

$$J_n \equiv X_n^* X_n = \|X_n\|^2 \tag{9}$$

then it is bounded as follows

$$\|X_n\| < \kappa \|X_{opt}\| \qquad \kappa = \beta + \upsilon\vartheta\bar{\sigma}(A)\frac{\vartheta}{\alpha - \vartheta} \tag{10}$$

where α is a free parameter ($\alpha > \vartheta$), and β, υ, and ϑ are given by the expressions

$$\beta \equiv \left\{ \begin{array}{l} \min\limits_{\gamma>0} \gamma: \\ \mu_\Delta(S(G,W)) < 1, \\ W \equiv \begin{bmatrix} \alpha A & A \\ \frac{\alpha}{\gamma} I & \frac{1}{\gamma} I \end{bmatrix}, \\ \Delta = \begin{bmatrix} \Delta_s & \\ & \Delta_f \end{bmatrix}, \ \Delta_f \in C^{n\times n} \end{array} \right\} \tag{11a}$$

$$\upsilon \equiv \left\{ \begin{array}{l} \min\limits_{\gamma>0} \gamma : \\ \mu_\Delta\left(\begin{bmatrix} G_{11} & G_{12} \\ \frac{1}{\gamma}G_{21} & \frac{1}{\gamma}G_{22} \end{bmatrix}\right) < 1, \\ \Delta = \begin{bmatrix} \Delta_s & \\ & \Delta_f \end{bmatrix}, \; \Delta_f \in C^{m\times n} \end{array} \right\} \quad (11b)$$

$$\vartheta \equiv \left\{ \begin{array}{l} \dfrac{1}{1-\min\limits_{0<\gamma<1}\gamma} : \\ \mu_\Delta\left(\mathrm{S}(G,V)\right) < 1, \\ V \equiv \begin{bmatrix} 0 & I \\ \frac{1}{\gamma}A & \frac{1}{\gamma}I \end{bmatrix}, \\ \Delta = \begin{bmatrix} \Delta_s & \\ & \Delta_f \end{bmatrix}, \; \Delta_f \in C^{m\times m} \end{array} \right\} \quad (11c)$$

Proof : See [6].

For large α, β can be considered a good approximation to κ. If this approximation holds, then $\mu_\Delta\left(\mathrm{S}(G,W)\right) < 1$ implies that $\|X_n\| < \beta\|X_{opt}\|$. A series expansion used in the derivation of Eqn. (10) requires that the stability condition, Eqn. (5), also be satisfied.

4 Synthesis of Robust Gain Matrices

The analysis results presented gives rise to a design algorithm for adaptive open loop control gain matrices [7]. The design procedure is as follows:

$$\underset{\substack{A,\mathcal{D}_L,\mathcal{D}_R,\tilde{q} \\ \mathcal{G}_L,\mathcal{G}_M,\mathcal{G}_R}}{\text{minimize}} \; q \; :$$

$$q \equiv \bar{\sigma}\left(\left(I+\mathcal{G}_L^2\right)^{-\frac{1}{4}}\left(\mathcal{D}_L\bar{\mathrm{S}}(A)\mathcal{D}_R^{-1} - j\tilde{q}\mathcal{G}_M\right)\left(I+\mathcal{G}_R^2\right)^{-\frac{1}{4}}\right), \quad (12)$$

$$q < \tilde{q}$$

where

$$\bar{\mathrm{S}} \equiv \begin{bmatrix} \mathrm{S}(G,V) & \\ & \mathrm{S}(G,W) \end{bmatrix} \quad (13)$$

$$\Delta = \begin{bmatrix} \Delta_s^1 & & & \\ & \Delta_f^1 & & \\ & & \Delta_s^2 & \\ & & & \Delta_f^2 \end{bmatrix} \quad \begin{array}{l} \Delta_s^1, \Delta_s^2 \in S_{\Delta_s} \\ \Delta_f^1 \in C^{m\times m} \\ \Delta_f^2 \in C^{n\times n} \end{array} \quad (14)$$

and V and W are as defined in Eqns. (8) and (11a).

If the minimization achieves $q<1$ then both the stability and performance robustness specifications are achieved by gain matrix A. Details of the synthesis procedure and proofs are given in [7].

5 Experimental Results

5.1 Magnetic Bearing Supported Rotor

A laboratory test rig with two radial magnetic bearings [5] was used to examine the robustness of the adaptive balancing algorithm. The rotor of this rig has a 12.7 mm diameter and a 508 mm bearing span. Eddy current position sensors are located vertically and horizontally near each bearing and the mid span disk. The rotor is supported using decentralized proportional-derivative control. The first critical speed of this rotor is at approximately 2700 rpm. Both the feedback control and the adaptive open loop algorithm were implemented in C on a digital controller designed and built at the University of Virginia's Center for Magnetic Bearings. The digital controller is a 32 bit floating point machine using a Texas Instruments TMS320C30 digital signal processor.

5.2 Model for Robustness Analysis and Synthesis

The rotor was modeled as an axisymmetric shaft with 13 mass stations using standard rotordynamic methods. The digital controller feedback transfer functions were obtained via a Tustin transformation of the difference equations. The switching amplifiers and sensors were modeled as constant gains. The actuator gains and bandwidths, bearing negative stiffness, and flexible coupling stiffness and damping were determined through a combination of physical modeling and parameter estimation based on numerical minimization of the error between experimental frequency response and model frequency response. The final model used in the synthesis procedure had 16 states.

The convergent control with the nominal system optimal gain matrix had excellent robustness with respect to a large number of variations for the experimental rotor. One variation in the system which produces a measurable difference between optimal performance and that obtained using the nominal system optimal gain matrix was rotor operating speed. Although rotor speed can be easily measured, it will be treated here as an uncertainty for the purpose of testing the theory presented. Treating the operating speed as uncertain parameter is also interesting as a method for developing very simple convergent controllers that do not need to be gain scheduled with respect to operating speed [9].

5.3 Stability Robustness Analysis Applied to Nominal System Optimal Gain Matrix

The nominal system optimal gain matrix was determined for the rotor at 3400 rpm from experimental measurements. This gain matrix was then used by the adaptive open loop control when the rotor was at other operating speeds. With the nominal system optimal gain matrix, the adaptation process was stable when the operating speed was between 2950 and 4300 rpm. The experiments performed yielded the values of the performance function without convergent control, with the nominal system optimal gain matrix, and with optimal control.

The stability robustness tests were applied to this problem to see if theory would predict the on-set of adaptation instability at 2950 rpm, a -14% change in operating speed from the nominal 3400 rpm. The stability robustness analysis predicts that the adaptation process will becomes unstable for variations of ±14%. This demonstrates that the stability tests can yield very accurate predictions of the tolerable uncertainty or variation *even for highly structured uncertainties.*

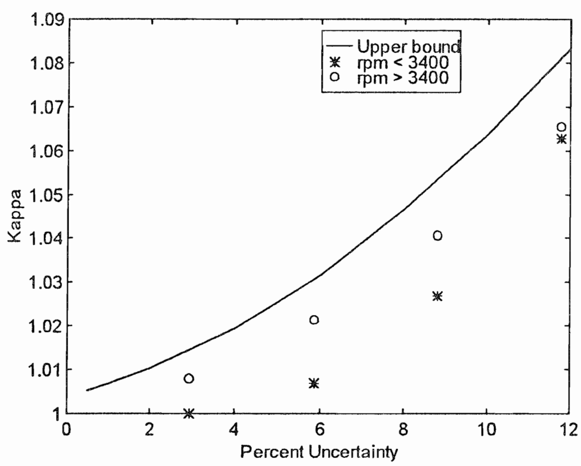

Fig. 1: Bound on worst case performance and experimental results

The performance robustness analysis predicts the bound on worst case performance shown in Figure 1 as a function of uncertainty in operating speed. Also shown in this figure are the experimentally determined performances for both negative and positive variations in operating speed. From a brief consideration of this plot, one might assume that the bound on performance is not tight. However, this experimental data was obtained for the rotor in only a single state of imbalance. The bound shown is for the worst case imbalance. Thus, the experimental results do not necessarily indicate any looseness of the bound.

5.4 Synthesized Gain Matrices

The synthesis procedure was applied to the problem considered and three gain matrices were designed. The goals of each of the three synthesis procedures are summarized in Table 1. In each case, the objective was to find a gain matrix which resulted in a larger range of stable operating speeds than the nominal system optimal gain matrix without sacrificing too much performance. For all three synthesis procedures, a convergence rate goal of $\varepsilon_c = 1$ was specified over the operating speed range. Recall that the nominal system optimal gain matrix produced unstable adaptation for a -14% variation in operating speed.

Syn.	Operating Speed Range (rpm)	Operating Speed Variation	Performance Goal |Xn| / |Xopt|
I	2720 - 4080	+/- 20 %	1.17
II	2550-4250	+/- 25%	1.26
III	1870 - 4930	+/- 45%	1.51

Table 1: Goals of synthesis

Each of the synthesized gain matrices were implemented on the test rig's controller and a series of experiments were conducted over a large operating speed range. Thus, a stable range of operating speeds was determined for each gain matrix. These results are summarized in Table 2. The results presented are the stable values inclusive; that is, the convergent control algorithm was stable for all the speeds tested in the range including the range's endpoints. Instability occurred for test speeds outside of this range. Tests were not conducted below 1800 rpm or above 4750 rpm; the later case due to instrumentation issues of the keyphasor.

Note that the synthesis procedure was quite successful in improving the stability robustness of the gain matrix to the variation in operating speed. For all three synthesized gain matrices, the range of stable variation achieved was as large or larger than the stability robustness specified during design (compare Tables 1 and 2). The results of the Synthesis III gain matrix are quite remarkable. The convergent control was stable over a range of operating speeds that includes two modes of the system (a threefold improvement over NSO).

Gain Matrix	Stable Range (rpm)	Stable Variation
NSO	3000 - 4300	- 12%, +26%
Syn. I	2550 - 4300	-25%, +26%
Syn. II	2550 - 4300	-25%, +26%
Syn. III	1800 - 4750 *	-47%, +40%

* total range tested

Table 2: Experimental stability robustness

The steady state vibration vector norm with optimal control, with the nominal system optimal gain matrix, and with each of the synthesized gain matrices are shown in Figures 2. Also shown is the uncontrolled synchronous vibration. The results for Synthesis II are not presented since they are nearly identical to those of Synthesis I.

All of the gain matrices tested resulted in a significant decrease in the peak vibration vector norm over the range of variation in operating speed. The performance robustness of the Synthesis I and II matrices was very similar to that of the nominal system optimal gain matrix, however, the stability range was significantly improved. For the Synthesis III gain matrix, the performance was the same or better than the uncontrolled performance over the entire range tested.

Another series of experiments were performed with a one gram balancing weight placed at the rotor midspan. This changed not only the state of rotor imbalance but also its distribution along the rotor. Thus, the direction of the uncontrolled vibration vector X_0 is changed as well as its magnitude. The two sets of experiments performed are referred to as Case 1 (no balancing weight added) and Case 2 (with balancing weight). The results of both sets of experiments are summarized in Table 3 along with the synthesis specifications. In all of the tests, the experimental performance was very close to the specification employed in synthesis. This result is a very strong verification of the effectiveness of the synthesis procedure.

Gain Matrix	Synthesis Specification		Perf. Achieved |Xn| / Xopt|	
	Speed Range (rpm)	Perf. Goal |Xn| /|Xopt|	Case 1	Case 2
Syn. I	2720 - 4080	1.17	1.20*	1.17
Syn. II	2550 - 4250	1.26	1.26	1.25
Syn. III	1870 - 4930	1.51	1.58♦	1.58♦

* maximum of data over a slightly larger range than specified
♦ smaller speed range than specified; instrumentation prevented testing over 4750 rpm

Table 3: Specification and experimental results for synthesized gain matrices

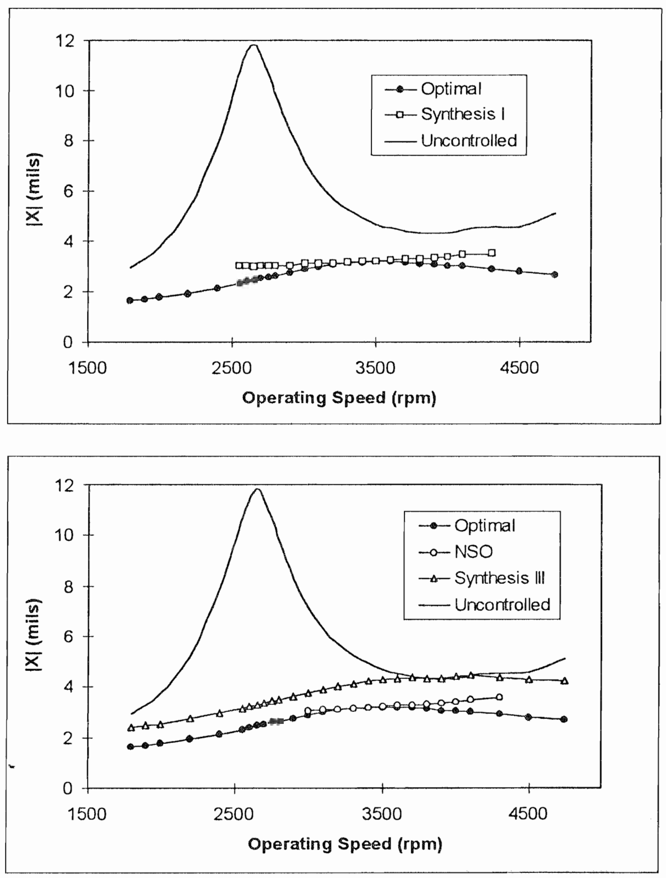

Fig. 2: Steady state vibration norm with various gain matrices

The steady state vibration normalized by the optimal vibration, $\|X_n\|/\|X_{opt}\|$, for each of the gain matrices tested is presented in Figure 3 for Case 1. Note that the Synthesis I and Synthesis II gain matrices have sacrificed very little nominal performance (3400 rpm) to achieve greater stability robustness than the nominal system optimal gain matrix. In contrast, the Synthesis III gain matrix achieves its very high stability robustness (±45%) by sacrificing the nominal performance.

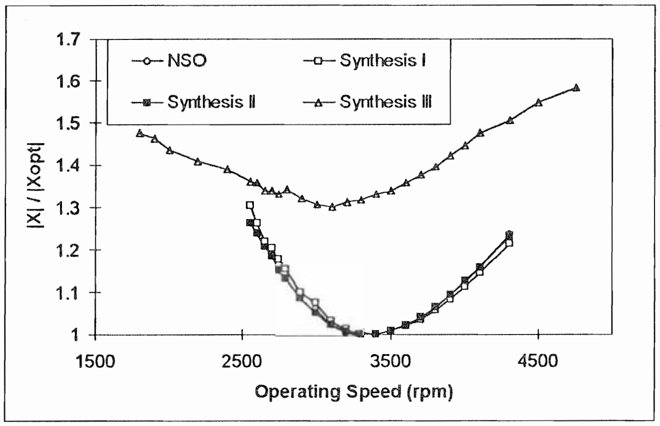

Fig. 3: Normalized performance for gain matrices tested

6 Conclusions

The robustness of adaptive open loop control algorithms for the suppression of the synchronous vibration of rotating machinery can be easily examined using the analysis methods presented. The experimental results demonstrate that the stability robustness analysis method yielded a very accurate prediction of the tolerable variation in a parameter (operating speed) that appears in a highly structured fashion in the system's dynamics. The performance robustness bounds obtained also accurately characterized the true degradation in performance with variation in the parameter. Furthermore, experimental results demonstrate that gain matrices found from the synthesis procedure presented resulted in a significant and predictable improvement in measured robustness of the synchronous vibration control process.

References

[1] H. Haberman and M. Brunet, "The Active Magnetic Bearing Enables Optimum Damping of Flexible Rotors", ASME Paper 84-GT-117, 1984.

[2] C.R. Burrows and M.N. Sahinkaya, "Vibration Control of Multi-Mode Rotor-Bearing Systems", *Proceedings of the Royal Society of London*, Vol. 386, pp. 77-94, 1984.

[3] R. Herzog, P. Buhler, C. Gahler, and R. Larsonneur, "Unbalance Compensation Using Generalized Notch Filters in the Multivariable Feedback of Magnetic Bearings", to appear in *IEEE Transactions on Control System Technology*, Sept. 1996.

[4] B. Shafai, S. Beale, P. LaRocca, and E. Cusson, "Magnetic Bearing Control Systems and Adaptive Forced Balancing", *IEEE Control Systems*, Volume 14, No. 2, pp. 4-13, April 1994.

[5] C. Knospe, R. Hope, S. Fedigan, and R. Williams, "Experiments in the Control of Unbalance Response Using Magnetic Bearings", *Mechatronics*, Vol. 5, No. 4, p.p. 385-400 1995.

[6] C. Knospe, S. Tamer, and S. Fedigan, "Robustness of Adaptive Rotor Vibration Control to Structured Uncertainty", to appear in *ASME Journal of Dynamic Systems,Measurement, and Control*, 1996.

[7] C. Knospe, S. Tamer, and S. Fedigan, "Synthesis of Robust Gain Matrices for Adaptive Rotor Vibration Control", submitted to *ASME Journal of Dynamic Systems, Measurement, and Control*, 1995.

[8] J. Doyle, A. Packard, and K. Zhou, Review of LFTs, LMIs and μ. *Proceedings of the 30th IEEE Conference on Decision and Control*, England, pp 1227-1232, 1991.

[9] C. Knospe, S. Tamer, and R. Fittro, "Rotor Synchronous Response Control: Approaches for Addressing Speed Dependence" , submitted to the *Journal of Vibration and Control*, 1996.